DOI: 10.1002/ejic.201000778

Fabrication of and Drug Delivery by an Upconversion Emission Nanocomposite with Monodisperse LaF_3:Yb,Er Core / Mesoporous Silica Shell Structure

Yifei Yang,[a] Yuqiu Qu,[a,b] Junwei Zhao,[a,b] Qinghui Zeng,[a] Yingying Ran,[a,b] Qingbin Zhang,[a,b] Xianggui Kong,*[a] and Hong Zhang*[c]

Keywords: Upconversion / Mesostructure / Drug delivery / Luminescence / Nanoparticles

Monodisperse, uniform, encapsulated mesoporous silica nanocomposites with a LaF_3:Yb,Er core and a mesoporous silica shell structure, which still exhibit green upconversion photoluminescence (PL) under 980 nm irradiation, have been successfully synthesized and investigated as potential drug delivery systems by using ibuprofen (IBU) as model drug.

Introduction

Mesoporous silica has been extensively studied with regard to its potential application in catalysis, optical devices, separation technology, drug delivery, and dye lasers,[1] ever since the discovery of ordered mesoporous M41S silica in 1992.[2] In recent years, its role in drug vehicles has received noticeable attention considering its superior properties, such as high surface area, large pore volume, uniform porosity, and excellent biocompatibility. In drug delivery with mesoporous silica,[3] the loading was realized by adsorption or capillary filling, and the release profiles were generally adjusted by monitoring the size and surface chemistry of the pores.

Meanwhile, with the development of nanoscience and nanotechnology, biofunctional nanocomposites with an incorporated robust framework to give multifunctional capabilities have been used for (multimodal) imaging implemented in simultaneous diagnosis and therapy[4]. There have been some reports[5] on the composites of photoluminescent materials and mesoporous silica for drug delivery; however, few of them tested these upconversion materials as drug delivery fields. In the upconversion materials, rare earth ions are embedded in a crystalline matrix. Recently, upconversion emission in terms of absorption of two or more lower-energy photons followed by emission of a higher energy photon has attracted much attention due to the availability of low-cost near-infrared laser diodes.[6] In biological tissues, the optical transmission window is approximately in the near-infrared (NIR) range,[7] which allows for deeper light penetration, lower autofluorescence and photodamage, reduced light scattering, and increased image contrast. Furthermore, the emission of upconversion materials contains sharp lines characteristic of atomic transitions in a well-ordered matrix. Using different rare earth dopants, a large number of distinctive emission spectra can be obtained, because of the rich energy levels of rare earth ions. As a result, rare-earth-doped upconversion materials might be multifunctional materials whose photoluminescence (PL) could be used for biolabeling, detection, and imaging in the future. In this context, nanocomposites combined with upconversion nanoparticles (UCNPs) and mesoporous silica would be a novel PL drug delivery vehicle.

Here, we report a scheme to fabricate core/shell nanocomposites with a silica-coated LaF_3:Yb^{3+},Er^{3+} nanoparticle core and a mesoporous silica shell, which are potential photocontrollable drug vehicles and bioimaging probes. LaF_3 is selected as core system, because of its special advantages such as low phonon energy, long luminescence lifetimes, and so on.[8] It was shown that the UCNPs with core/shell structure allow the process of drug release to be easily identified, tracked, and monitored by luminescence.

Results and Discussion

Structure of LaF_3:Yb^{3+},Er^{3+}@*n*SiO_2@*m*SiO_2 Microspheres

The initial LaF_3:Yb^{3+},Er^{3+} particles were prepared by the hydrothermal method as described.[9] Transmission electron microscopy (TEM) reveals that these particles are uniform with a mean diameter of approximately 13 nm (Figure 1a). The polycrystallinity of LaF_3:Yb^{3+},Er^{3+} nanoparticles was confirmed by selected area electron diffraction (SAED) patterns and X-ray diffraction analysis (Figure 3).

[a] Key Laboratory of Excited-State Process, Changchun Institute of Optics Fine Mechanics and Physics, Chinese Academy of Sciences,
Changchun 130033, P. R. China
[b] Graduate School of Chinese Academy of Sciences,
Beijing 100049, P. R. China
[c] Van 't Hoff Institute for Molecular Sciences, University of Amsterdam,
Amsterdam, Netherlands

Supporting information for this article is available on the WWW under http://dx.doi.org/10.1002/ejic.201000778.

These uniform cores result in a narrow distribution of the final particle sizes. In Figure 1b, the image of the obtained silica-coated initial LaF_3:Yb^{3+},Er^{3+} particles shows that the silica coating is also uniform with a thickness of about 12 nm. With this dense coating, the LaF_3:Yb^{3+},Er^{3+} cores would be protected into the mother system under biological conditions rather than rapidly dissolved through the pores of the mesoporous shell. CTAB surfactant molecules used as the template were assembled into a hexagonal array for directing the formation of mesoporous silica according to a liquid crystal templating mechanism on the LaF_3:Yb^{3+},Er^{3+}core/SiO_2 shell microspheres. The removal of CTAB was verified by Fourier transform infrared (FTIR) spectrometric analysis (Figure 2). For the LaF_3:Yb^{3+}, Er^{3+}@$n$$SiO_2$@CTAB/$SiO_2$, the bands observed in the 2800–3000 cm^{-1} region are attributed to the vibrations of $–CH_2$ groups of the CTAB templates. After mild treatment (three extractions with acetone), no absorption peaks were observed in the range 2800–3000 cm^{-1} for the LaF_3:Yb^{3+}, Er^{3+}@$n$$SiO_2$@$m$$SiO_2$ microspheres, suggesting that the CTAB templates were completely removed.

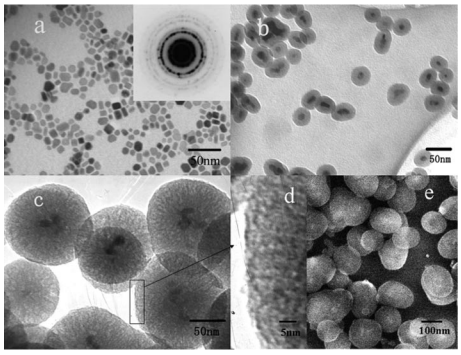

Figure 1. TEM images of (a) LaF_3:Yb^{3+},Er^{3+} particles, (b) LaF_3:Yb^{3+},Er^{3+}@$n$$SiO_2$, (c,d) LaF_3:Yb^{3+},Er^{3+}@$n$$SiO_2$@$m$$SiO_2$ microspheres; (e) SEM image of LaF_3:Yb^{3+},Er^{3+}@$n$$SiO_2$@$m$$SiO_2$ microspheres.

After successful removal of the organic group of CTAB by extraction, which served as the surfactant during the growth process of the mesoporous layer, the mesoporous silica shell was evenly formed with a roughly uniform thickness of about 47 nm over the silica-coated LaF_3:Yb^{3+},Er^{3+} core. The pores are revealed to be randomly arranged in the mesoporous silica shell. The TEM image (Figure 1c) clearly demonstrates the formation of the LaF_3:Yb^{3+}, Er^{3+}@$n$$SiO_2$@$m$$SiO_2$ nanoparticles. Wormhole-like mesopores are observed in the silica shells (Figure 1d). The formed LaF_3:Yb^{3+},Er^{3+}@$n$$SiO_2$@$m$$SiO_2$ nanoparticles reveal a quite complex pore structure, where the mesochannels do not align over the entire nanoparticle but are distributed in all directions randomly, starting at the inner part of the sphere and going out to the external edge.

A typical sandwich structure with a LaF_3:Yb^{3+},Er^{3+} core, a nonporous silica layer in the middle layer, and an ordered mesoporous silica phase with worm-like mesochannels in the outer layer can be clearly observed. The SEM

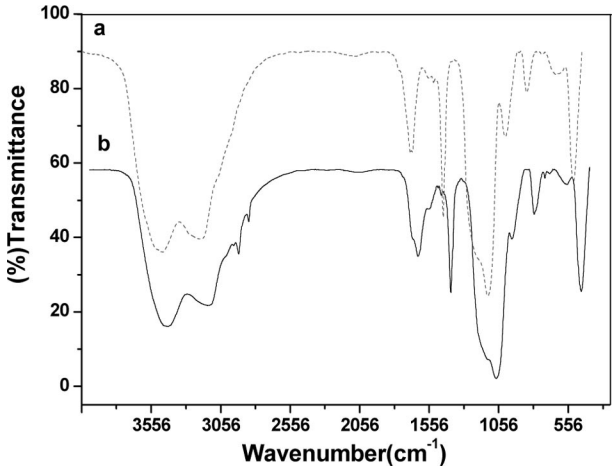

Figure 2. FTIR spectra of (a) as-made LaF_3:Yb^{3+},Er^{3+}@$n$$SiO_2$@CTAB/$m$$SiO_2$ before treatment with acetone and (b) LaF_3:Yb^{3+},Er^{3+}@$n$$SiO_2$@$m$$SiO_2$ microspheres after acetone extraction.

image (Figure 1e) shows that the particles are spherical in shape and uniform in dimension with diameters of approximately 130 nm. The dynamic light scattering (DLS) image (Figure S1 in the Supporting Information) shows that the LaF_3:Yb,Er core/mesoporous silica shell nanocomposites are well-dispersed, with a mean hydrodynamic diameter of 150 nm. The particle size observed with electron microscopy is slightly smaller than the hydrodynamic diameter measured by DLS. This observation may be due to the occasional weak aggregation of the particles. In our synthesized system, the silica oligomers interact with the CTAB template via Coulomb forces, and both of them assemble cooperatively on the surface of the LaF_3:Yb^{3+},Er^{3+}@silica microspheres to form the ordered mesostructure. The mesoporous orientation may result from the preferred alignment fashion of the rod-shaped silicate/CTAB complexes on the carved surface of the LaF_3:Yb^{3+},Er^{3+}@$n$$SiO_2$ microspheres, which can effectively decrease the surface energy in the synthesis system (Scheme 1). The obtained microspheres have an interesting microstructure, which is very useful. The silica coating on the initial LaF_3:Yb^{3+},Er^{3+} particles could protect the UCNPs from etching under harsh application conditions. With regard to the mesoporous silica shell, it

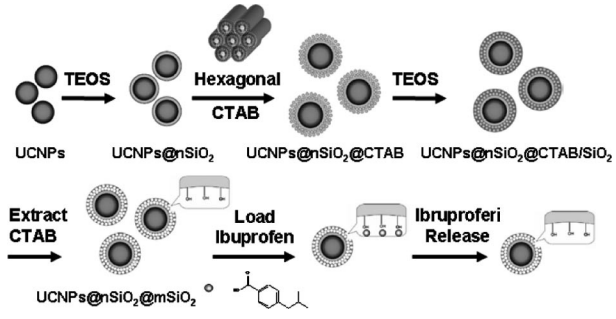

Scheme 1. Schematic view of the synthesis of LaF_3:Yb^{3+},Er^{3+}@$n$$SiO_2$@$m$$SiO_2$ microspheres and the subsequent loading and release of the ibuprofen (IBU) drug.

does not only offer high surface area for the derivation of numerous functional groups but also provides a large accessible pore volume for the adsorption, encapsulation, and release of drug molecules and even functional nanoparticles (e.g., quantum dots). It is remarkable that the mesoporous channels of the microspheres are readily accessible, favoring the adsorption and release of the drug ibuprofen when triggered by an external stimulus.

The wide-angle XRD patterns (Figure 3A) of LaF_3:Yb^{3+},Er^{3+} and LaF_3:Yb^{3+},Er^{3+}@$n$$SiO_2$@$m$$SiO_2$ show that the microspheres have the same diffraction peaks as those of the parent LaF_3:Yb^{3+},Er^{3+} particles, suggesting that the LaF_3:Yb^{3+},Er^{3+} particles are well retained in the silica matrix. Furthermore, the low-angle XRD pattern reveals that the LaF_3:Yb^{3+},Er^{3+}@$n$$SiO_2$@$m$$SiO_2$ microspheres have hexagonal mesoporous symmetry (Figure 3B). Because the mesoporous channels are perpendicular to the surface, ethanol can lower the hydrolysis and condensation rate of tetraethyl orthosilicate (TEOS) and favor coating and curving. The microspheres possess short-range mesoscopic ordering character. The absorption/desorption isotherms of N_2 exhibit IV-type curves for the microspheres (Figure 4). The mesoporous size distribution (Figure 4, inset) exhibits a sharp peak centered at a mean value of 6.4 nm, indicating a uniform mesopore. The BET surface area and total pore volume are calculated to be 126.6 $m^2 g^{-1}$ and 0.07 $cm^3 g^{-1}$, respectively.

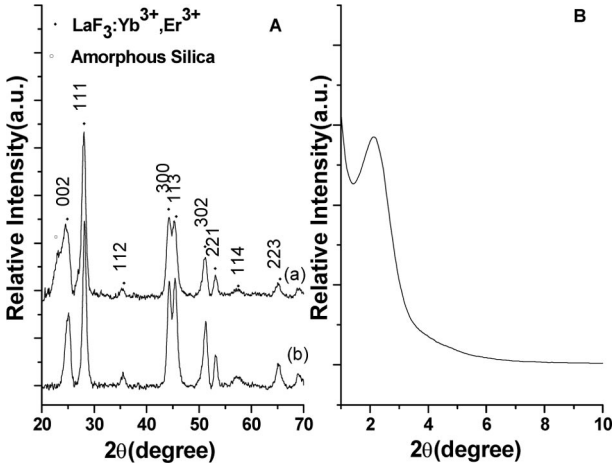

Figure 3. (A) Wide-angle XRD patterns of (a) LaF_3:Yb^{3+},Er^{3+}@$n$$SiO_2$@$m$$SiO_2$ microspheres and (b) LaF_3:Yb^{3+},Er^{3+} nanoparticles. (B) The low-angle XRD pattern of the LaF_3:Yb^{3+},Er^{3+}@$n$$SiO_2$@$m$$SiO_2$ microspheres.

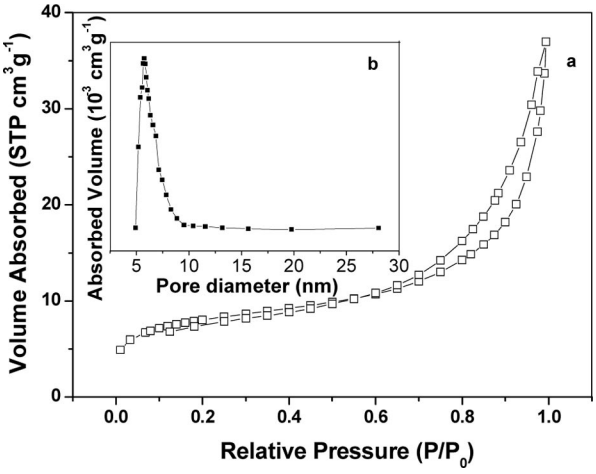

Figure 4. (a) N_2 adsorption/desorption isotherms for LaF_3:Yb^{3+},Er^{3+}@$n$$SiO_2$@$m$$SiO_2$ microspheres; (b) pore-size distribution from the adsorption branch (inset).

Luminescence and Drug Delivery

The fluorescence spectrum of LaF_3:Yb^{3+},Er^{3+} nanoparticles and LaF_3:Yb^{3+},Er^{3+}@$n$$SiO_2$@$m$$SiO_2$ microspheres is shown in Figure 5a. The pure upconversion emission, excited with a 980 nm continuous-wave diode laser irradiation, has been observed even with the naked eye. As shown in Figure 5, the upconversion emission spectrum of initial LaF_3:Yb^{3+},Er^{3+} and LaF_3:Yb^{3+},Er^{3+}@$n$$SiO_2$@$m$$SiO_2$ microspheres have similar peak positions, indicating that the local crystalline environments are identical before and after silica coating. There are three emission peaks at 517, 536, and 651 nm, which are assigned to the 2H11/2 to 4I15/2, 4S3/2 to 4I15/2, and 4F9/2 to 4I15/2 transitions of erbium, respectively. Under 980 nm excitation, Er^{3+} absorbs one photon and its ground-state (4I15/2) electron is excited to the 4I11/2 level. The second photon promotes the electron to the 4F7/2 level. The excited electron decays first nonradiatively to the 2H11/2, 4S3/2, and 4F9/2 levels. When it decays further to the ground state, emission at 518, 537, and 652 nm occurs. The silica-coated microspheres show a little decrease in fluorescence intensity relative to the uncoated microspheres. This mesoporous structure has less effect on luminescence intensity, the luminescence intensity ratio (I540/I654) of the fluorescence spectra ranging from

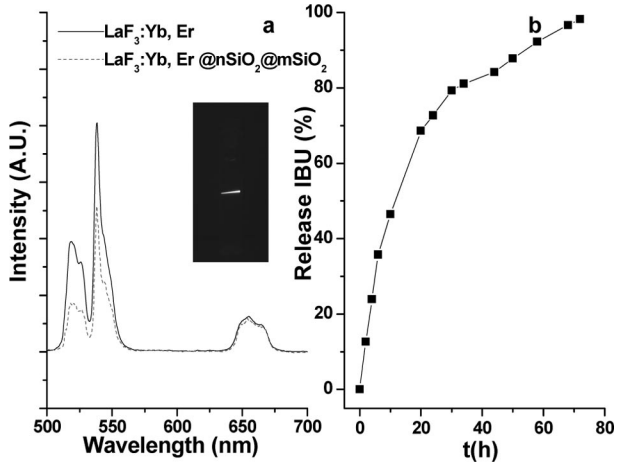

Figure 5. (a) Luminescence spectrum of LaF_3:Yb^{3+},Er^{3+} nanoparticles and LaF_3:Yb^{3+},Er^{3+}@$n$$SiO_2$@$m$$SiO_2$ microspheres excited with a 980 nm laser; inset: upconversion luminescence of LaF_3:Yb^{3+},Er^{3+}@$n$$SiO_2$@$m$$SiO_2$ solution under continuous-wave excitation at 980 nm. (b) Cumulative ibuprofen release from the ibuprofen–LaF_3:Yb^{3+},Er^{3+}@$n$$SiO_2$@$m$$SiO_2$ system in the release medium of a simulated body fluid (SBF).

0.73 to 0.68 is attributed to the silica coating as shown in Figure 5a, which means that the upconversion mechanism is not affected by the silica coating processes (Figure 6).

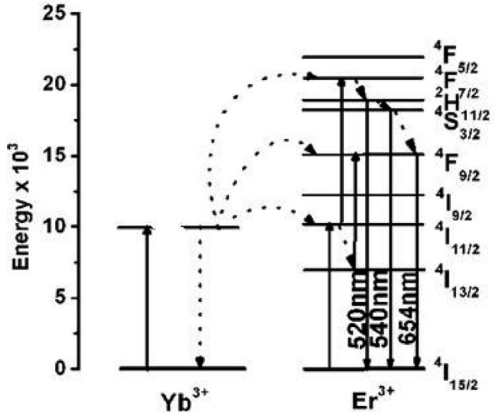

Figure 6. Schematic energy level diagrams of the Er^{3+} and Yb^{3+} dopant ions in mesostructured LaF_3: 10 wt.-% Yb^{3+}, 2 wt.-% Er^{3+} nanoparticles and the upconversion mechanism excited by a 980 nm laser diode.

To explore the capability of the synthesized particles as drug carrier, ibuprofen was introduced into the pores of LaF_3:Yb^{3+},Er^{3+}@$n$$SiO_2$@$m$$SiO_2$. Ibuprofen is a well-known nonsteroidal anti-inflammatory drug and has been widely used for the treatment of inflammation, pain, and rheumatism. However, this drug has a short biological half-life (2 h) with molecular weights of about 1000 Da.,[10] which makes it a suitable candidate for sustained or controlled drug delivery. The characteristic pore-filling step disappears in the N_2 adsorption isotherm (Figure 4) after ibuprofen is stored, and the pore volume decreases by 70%, which indicates that most of the pores have been filled. The amount of uptake of ibuprofen is approximately 12 wt.-%. Figure 5b shows the release behavior of ibuprofen in SBF over 70 h at 37 °C. The release process is relatively fast during the first 24 h, but decreases with time and reaches a value of 98% after 72 h.

Conclusions

In summary, we have successfully fabricated a novel kind of upconversion luminescence core/mesoporous silica shell microspheres with a uniform particle diameter of 130 nm. The inner luminescence core LaF_3:Yb^{3+}, Er^{3+}@$n$$SiO_2$@$m$$SiO_2$ endues the nanoparticles with upconversion properties. The outer mesoporous silica shell has a high enough surface area and pore volume. Ibuprofen can be stored in the channels of the microspheres, and most of the drug molecules incorporated can be released to the SBF in 70 h. The abundant silanol groups present on the surface offer exceptional support for particle functionalization, while the mesoporous structure allows the confinement and control of the diffusion of molecules. Upconversion nanoparticles give optical properties to these composites. Therefore, we expect that this material may be applicable in targeted drug delivery, bioimaging, and biosensing.

Experimental Section

Materials: All the reagents for synthesis, tetraethoxysilane [$(C_2H_5O)_4Si$, TEOS, Aldrich], Igepal CO-520 [$(C_2H_4O)_n$·$C_{15}H_{24}O$, $n \approx 5$, Aldrich], cetyltrimethylammonium bromide (CTAB, Beijing Chemical Regent Company), NaF (Beijing Chemical Regent Company), ethanol (Beijing Chemical Regent Company), oleic acid (Beijing Chemical Regent Company), hexane (Beijing Chemical Regent Company), cyclohexane (Beijing Chemical Regent Company), acetone (Beijing Chemical Regent Company), ammonia solution (28%, Beijing Chemical Regent Company), hydrochloric acid (36–38%, Beijing Chemical Regent Company), and NaOH (Beijing Chemical Regent Company) were received without further purification.

Preparation of LaF_3:Yb^{3+},Er^{3+} Nanoparticles: In a typical procedure, NaF (3 mmol), water (12 mL), ethanol (9 mL), and oleic acid (3 mL) were mixed together under agitation to form a homogeneous solution and heated to 75 °C for 1 h. Then, an aqueous solution of rare earth nitrates [$Ln(NO_3)_3$, Ln: 85 mol-% La, 12 mol-% Yb, 3 mol-% Er] (1 mmol in total) was added to the heated homogeneous solution, and the magnetic stirring was continued for about 1 h at 75 °C. The solution was transferred to a 60 mL autoclave, sealed, and hydrothermally treated at 120 °C for 12 h. Consequently, the products that were deposited at the bottom of the vessel after the autoclave was allowed to cool down to room temperature naturally were collected with hexane, and ethanol was added. The precipitates were separated by centrifugation, washed with ethanol in sequence several times, and then stored in cyclohexane (3 mL, 0.3 mmol/mL).

Preparation of Silica-Coated LaF_3:Yb^{3+},Er^{3+} Nanoparticles: Silica coating was performed through the formation of a water-in-cyclohexane reverse microemulsion. Typically, Igepal CO-520 (1.2 mL) was added to the as-prepared solution of LaF_3:Yb^{3+},Er^{3+} nanoparticles (30 mL, 1.33×10^{-2} mmol/mL). Ammonia solution (195 μL) and TEOS (150 μL) were then added consecutively whilst stirring to form a transparent solution of reverse microemulsion. Silica-coated LaF_3:Yb^{3+},Er^{3+} nanoparticles with an overall size of 37 nm were obtained after reaction for 24 h at room temperature. When the desired particle size was achieved, ethanol was added to disrupt the reverse microemulsion, and the LaF_3:Yb^{3+},Er^{3+}@$n$$SiO_2$ nanoparticles were extracted into the ethanol phase; then they were collected by centrifugation and redispersed in water.

Preparation of LaF_3:Yb^{3+},Er^{3+}@$n$$SiO_2$@$m$$SiO_2$ Microspheres: After being stirred at room temperature for 1 h, the LaF_3:Yb^{3+},Er^{3+}@$n$$SiO_2$ microspheres (0.4 mmol) were separated and washed with ethanol and water, and redispersed in a mixed solution containing CTAB (40 mg, 0.110 mmol), deionized water (10.6 mL), concentrated NaOH solution (120 μL, 2 M), and ethanol (2 mL). The mixed solution was homogenized for 0.5 h to form a uniform dispersion. TEOS (250 μL, 1.116 mmol) was added dropwise to the dispersion with continuous stirring. After reaction for 6 h, the product was collected by centrifugation and washed with ethanol and water four times repeatedly. Finally, the purified microspheres were redispersed in acetone (60 mL) and heated at reflux at 80 °C for 48 h to remove the CTAB template. The extraction was repeated three times, and the LaF_3:Yb^{3+},Er^{3+}@$n$$SiO_2$@$m$$SiO_2$ microspheres were washed with deionized water to obtain the final products.

Drug Storage and Release: The typical drug storage and release experiments in vitro were performed as follows: a certain amount of LaF_3:Yb^{3+},Er^{3+}@$n$$SiO_2$@$m$$SiO_2$ was added into a hexane solution of ibuprofen (40 mg/mL). The suspension was stirred for 24 h

while hexane evaporation was prevented. Then the LaF_3:Yb^{3+},Er^{3+}@$n$$SiO_2$@$m$$SiO_2$ particles loaded with the drug were separated. An aliquot (1 mL) of the release medium solution was removed for analysis at given time intervals and replaced with the same volume of fresh preheated SBF at 37 °C. The ionic composition of the as-prepared SBF solution was similar to that of human body plasma with a molar composition of 142.0/5.0/2.5/1.5/147.8/4.2/1.0/0.5 for Na^+/K^+/Ca^{2+}/Mg^{2+}/Cl^-/HCO_3^-/HPO_4^{2-}/SO_4^{2-} (pH = 7.4). The medium solution (1.0 mL) extracted for analysis was diluted to 4 mL with SBF and analyzed by UV/Vis spectroscopy at 273 nm.

Characterizations: The formation and quality of the compounds were checked at room temperature by using a D/max-IIB X-ray Theta-Theta diffractometer with Cu-K_α radiation (λ = 0.15406 nm). The microstructure, particle size, and particle distribution studies were performed with a transmission electron microscope (TEM, JEM-1011, JEOL, Japan). The size and morphology of the products were characterized by field emission scanning electron microscopy (FESEM, Hitachi, S-4800). Nitrogen adsorption/desorption analysis was performed by using a Micromeritics ASAP 2010 M apparatus. The specific surface area was determined by the Brunauer–Emmett–Teller (BET) method. The removal of CTAB was verified by Fourier transform infrared (FTIR) spectroscopic analysis (FTS135, Bio-Rad, American). The mean hydrodynamic size and size distribution were determined by dynamic light scattering (DLS) with a Malvern Instruments Zetasizer 1000HSA. UV/Visible spectra of the ibuprofen release was taken with a Cary 500 UV/Vis spectrophotometer (VARIAN). The upconversion emission spectra were acquired by using a Jobin–Yvon LabRam Raman spectrometer system and a Peltier air-cooled CCD detector.

Supporting Information (see footnote on the first page of this article): Hydrodynamic diameter distribution of LaF_3:Yb^{3+}, Er^{3+}@$n$$SiO_2$@$m$$SiO_2$ microspheres in EtOH.

Acknowledgments

This project is financially supported by the National Natural Science Foundation of China (NSFC) grants 60771051, 10904142, 11004189 and the China Exchange Programme of the Koninklijk Nederlandse Akademie van Wetenschappen (KNAW).

[1] a) J. Y. Ying, C. P. Mehnert, M. S. Wong, *Angew. Chem. Int. Ed.* **1999**, *38*, 56–77; b) X. Y. Yang, Y. Han, K. F. Lin, G. Tian, Y. F. Feng, X. G. Meng, Y. Di, Y. C. Du, Y. L. Zhang, F. S. Xiao, *Chem. Commun.* **2004**, 2612–2613; c) F. Hoffmann, M. Cornelius, J. Morell, M. Fröba, *Angew. Chem. Int. Ed.* **2006**, *45*, 3216–3251; d) M. Vallet, F. Balas, D. Arcos, *Angew. Chem. Int. Ed.* **2007**, *46*, 7548–7558; e) L. Zhang, S. Z. Qiao, Y. G. Jin, H. G. Yang, S. Budihartono, F. Stahr, Z. F. Yan, X. L. Wang, Z. P. Hao, G. Q. Lu, *Adv. Funct. Mater.* **2008**, *18*, 3203–3212; f) M. Liong, B. France, K. A. Bradley, J. I. Zink, *Adv. Mater.* **2009**, *21*, 1684–1689.

[2] C. T. Kresge, M. E. Leonowicz, W. J. Roth, J. C. Vartuli, J. S. Beck, *Nature* **1992**, *359*, 710–712.

[3] S. W. Song, K. Hidajat, S. Kawi, *Chem. Commun.* **2007**, 4396–4398.

[4] a) M. Liong, J. Lu, M. Kovochich, T. Xia, S. G. Ruehm, A. E. Nel, F. Tamanoi, J. I. Zink, *ACS Nano* **2008**, 2,889–896; b) J. Kim, H. S. Kim, N. Lee, T. Kim, H. Kim, T. Yu, I. C. Song, W. K. Moon, T. Hyeon, *Angew. Chem. Int. Ed.* **2008**, *47*, 1–5; c) W. R. Zhao, J. L. Gu, L. X. Zhang, H. R. Chen, J. L. Shi, *J. Am. Chem. Soc.* **2008**, *130*, 28–29; d) W. R. Zhao, H. R. Chen, Y. S. Li, L. Li, M. D. Lang, J. L. Shi, *Adv. Funct. Mater,.* **2008**, *18*, 2780–2788.

[5] a) P. P. Yang, S. S. Huang, D. Y. Kong, J. Lin, H. G. Fu, *Inorg. Chem.* **2007**, *46*, 3203–3211; b) J. W. Liu, A. S. Naughton, X. M. Jiang, C. J. Brinker, *J. Am. Chem. Soc.* **2009**, *131*, 1354–1355.

[6] J. H. Zeng, T. Xie, Z. H. Li, Y. D. Li, *Cryst. Growth Des.* **2007**, *7*, 2774–2777.

[7] a) R. Weissleder, *Nat. Biotechnol.* **2001**, *19*, 316; b) M. Nyk, R. Kumar, T. Y. Ohulchanskyy, E. J. Bergey, P. N. Prasad, *Nano Lett.* **2008**, *8*, 3834–3838.

[8] a) G. S. Yi, G. M. Chow, *J. Mater. Chem.* **2005**, *15*, 4460; b) S. Sivakumar, P. R. Diamente, F. C. J. M. van Veggel, *Chem. Eur. J.* **2006**, *12*, 5878.

[9] L. Y. Wang, R. X. Yan, Z. Y. Huo, L. Wang, J. H. Zeng, J. Bao, X. Wang, Q. Peng, Y. D. Li, *Angew. Chem. Int. Ed.* **2005**, *44*, 6054–6057.

[10] F. Highton, "The Pharmaceutics of Ibuprofen" in *Ibuprofen. A Critical Bibliographic Review* (Ed.: K. D. Rainsford), Taylor & Francis, London, **1999**, p. 53.

Received: July 17, 2010
Published Online: October 20, 2010

